

SAND2003-3866
Unlimited Release
Printed October 2003

**Chem-Prep PZT 95/5 for Neutron Generator Applications: The Effect
of Pore Former Type and Density on the Depoling Behavior of
Chemically Prepared PZT 95/5 Ceramics**

Pin Yang, Roger H. Moore, and Steve J. Lockwood
Ceramics and Glass Processing Department

Bruce A. Tuttle
Ceramic Materials Department

James A. Voigt
Chemical Synthesis and Nano-materials Department

Timothy W. Scofield
Neutron Generator Design Department

Sandia National Laboratories
P. O. Box 5800
Albuquerque, New Mexico 87185-0959

ABSTRACT

The hydrostatically induced ferroelectric(FE)-to-antiferroelectric(AFE) phase transformation for chemically prepared niobium modified PZT 95/5 ceramics was studied as a function of density and pore former type (Lucite or Avicel). Special attention was placed on the effect of different pore formers on the charge release behavior associated with the FE-to-AFE phase transformation. Within the same density range (7.26 g/cm^3 to 7.44 g/cm^3), results showed that ceramics prepared with Lucite pore former exhibit a higher bulk modulus and a sharper polarization release behavior than those prepared with Avicel. In addition, the average transformation pressure was 10.7% greater and the amount of polarization released was 2.1% higher for ceramics with Lucite pore former. The increased transformation pressure was attributed to the increase of bulk modulus associated with Lucite pore former. Data indicated that a minimum volumetric transformational strain of -0.42% was required to trigger the hydrostatically induced FE-to-AFE phase transformation. This work has important implications for increasing the high temperature charge output for neutron generator power supply units.

This work performed at Sandia National Laboratories supported by the U.S. Department of Energy's National Nuclear Security Administration under Contract Number DE-AC04-94AL85000.

ACKNOWLEDGEMENTS

The authors would like to acknowledge John Gieske, Diana Moore, Emily Rodman, Ted V. Montoya, Tom Spindle, Johnny Q. Rice, and Peter Manley for their support with elastic property measurement, powder synthesis, processing, and electrical testing. Support from Ronnie Stone, Scarlett M. DeNinno and the voltage-bar grinding and assembly team are also greatly appreciated.

TABLE OF CONTENTS

ABSTRACT.....	1
ACKNOWLEDGEMENTS.....	2
TABLE OF CONTENTS.....	3
LIST OF TABLES.....	4
LIST OF FIGURES.....	5
1. INTRODUCTION.....	6
1.1 Review of Previous Work.....	6
<i>1.1.1 Hydrostatically induced phase transformation characteristics.....</i>	<i>6</i>
<i>1.1.2 Effect of density and pore former on phase transformation.....</i>	<i>7</i>
2. EXPERIMENTAL PROCEDURE.....	7
3. RESULTS AND DISCUSSION.....	8
3.1 Density, Pore Former, and Bulk Modulus.....	9
3.2 Density, Pore Former, and Depoling Characteristics.....	10
3.3 Strain-Induced FE-to-AFE Phase Transformation.....	12
4. SUMMARY.....	13
REFERENCES.....	23

LIST OF TABLES

Tables	page
I. Sample Identification and Measured Density.....	14
II. The Effective Elastic Constant as a Results of the Effects of Piezoelectricity..	14
III. Young's Moduli of PZT 95/5 Ceramics of Different Density and Pore Former.....	14
IV. The Bulk Moduli of PZT 95/5 Ceramics of Different Density and Pore Former.....	15
V. The Average Density, Dielectric, and Depoling Properties of PZT 95/5 Ceramic with Different Size of Lucite Pore Former.....	15

LIST OF FIGURES

Figures	Page
1. Microphotograph of Avicel microcrystalline cellulose.....	16
2. Microphotograph of Lucite (PMMA), sieved through a 120 mesh screen.....	16
3. The pressure-volumetric strain response for the hydrostatically induced FE-to-AFE phase transformation of Nb modified PZT 95/5 ceramics.....	17
4. The polarization released behavior for the hydrostatically induced FE-to-AFE phase transformation of Nb modified PZT 95/5 ceramics	17
5. The effect of density on bulk modulus of poled PZT 95/5 ceramics with different pore formers.....	18
6. The depoling behavior of Nb modified PZT 95/5 with Avicel pore former hydrostatically loaded to (a) 482.65 MPa compared with PZT 95/5 loaded /unloaded sequentially to/from (b) 137.9, (c) 206.85, (d) 275.8, and (e) 483.65 MPa.....	18
7. The amount of polarization released during the loading and unloading cycle below the transformational pressure for Avicel containing PZT 95/5.	19
8. The general depoling behavior for Nb modified PZT 95/5 ceramics with different densities containing Avicel pore former.....	19
9. The general depoling behavior for Nb modified PZT 95/5 ceramics with different densities containing Lucite pore former	20
10. The depoling behavior for Nb modified PZT 95/5 ceramics with different size of Lucite pore former.....	20
11. The amount of polarization release as a function of pore former and bulk density for niobium modified PZT 95/5 ceramics.....	21
12. Depoling pressure as a function of pore former and bulk density for niobium modified PZT 95/5 ceramics.....	21
13. The correlation between the bulk modulus and transformation pressure for niobium modified PZT 95/5 ceramics with different pore formers.....	22

1. INTRODUCTION

The lead zirconate titanate (PZT) solid solution system has been studied extensively, particularly for ceramic with compositions near the morphotropic phase boundary where electromechanical properties are most pronounced.¹ As the composition in the PZT solid solution system shifts from the lead titanate rich region to the lead zirconate region, the tetragonal distortion reduces and ultimately leads to the appearance of a ferroelectric (FE) phase with rhombohedral symmetry. With further increase in Zr⁺⁴ content, the dipoles in the crystalline structure progressively change from a long-range-ordered configuration in the FE phase to a short-range-ordered configuration in the orthorhombic antiferroelectric (AFE) phase. This occurs at room temperature when the Zr/Ti ratio is near 95/5.¹ Near this composition, free energy differences between the high temperature rhombohedral FE phase, low temperature rhombohedral FE phase, and the orthorhombic AFE phase are very small.¹ Two delicate competing forces in these crystalline materials, namely a long-range interaction force and a short-range interaction force, driving the formation of a long-range-ordered structure or a short-range-ordered structure, can be greatly influenced by an external field^{2, 3} and small variations in chemical composition and lead stoichiometry.⁴ For example, an applied electrical field interacting with dipoles in the PZT 95/5 material favors the long-range-ordered FE phase, while hydrostatic pressure reduces the interionic distance and greatly enhances the short-range interactions.² Hence, the dielectric dipoles of a FE material in the adjacent cells couple together in an anti-parallel configuration under a hydrostatic pressure condition and transform into the short-range-ordered AFE phase. These characteristics for PZT close to the FE and AFE phase boundary lead to many interesting applications such as ceramic actuators^{5,6,7}, and shock-wave power supplies.^{8,9}

In this report, the effect of pore former on the FE-to-AFE phase transformation behavior under a hydrostatic condition in poled PZT 95/5 ceramics made from a chemically-prepared (chem.-prep) powder was examined.¹⁰ Pore former was added to the ceramic formulation to control the final sintered density of the ceramics. Two different pore formers, Avicel and Lucite, were used in this study. Avicel particles, a pharmaceutical grade of microcrystalline cellulose, were generally acicular in shape with length ranging from ~20 to 120 μm and diameters ranging from 5 to 40 μm (Figure 1). Lucite particles were made of polymerized methyl methacrylate with a spherical geometry and diameters range from 40 to 120 μm (Figure 2). Ceramics within the requisite density range were fabricated into MC3422 and MC4576 voltage bars for neutron generator power supplies

1.1 Review of Previous Work

1.1.1 *Hydrostatically induced phase transformation characteristics*

Zeuch and coworkers¹¹ demonstrated that PZT 95/5 ceramics subjected to hydrostatic pressure exhibit approximately linear volumetric strain behavior prior to the

FE-to-AFE phase transformation (Figure 3). The horizontal section of this strain-pressure curve represents a volumetric transformational strain of -0.74% when the ceramic transforms from a larger rhombohedral FE structure to a smaller orthorhombic AFE structure. This sudden volumetric strain change near 295 MPa (or triggered at a volumetric strain of 0.42%) is characteristic of a classic first order phase transformation. The linear relationship between the applied pressure and volumetric strain prior to and after the phase transformation corresponds to the bulk modulus of FE phase and AFE phase, respectively. Upon unloading, the transformational strain does not recover which indicates the transformation is irreversible at room temperature. During the hydrostatically induced FE-to-AFE phase transformation, the bound charge (or polarization) stored on the electrodes of poled FE ceramics is released as the dipoles in adjacent cells couple into an AFE configuration (this process is commonly referred as hydrostatic depoling). Figure 4 illustrates the typical charge release behavior of poled PZT 95/5 ceramics under hydrostatic compression (Figure 3 and Figure 4 depict data from the same material lot). Virtually all the bound charge on the electrodes is released during the phase transformation, which initiates at approximately 295 MPa.

1.1.2 Effect of density and pore former on phase transformation

Storz and Dungan¹² studied the electrical, and mechanical properties, as well as the shock-wave induced FE-to-AFE phase transformation (typically referred to as “functional testing”) behavior of mixed oxide PZT 95/5 ceramics as a function of pore former type and concentration. Bulk density, dielectric constant, remanent polarization, depoling pressure, depoling charge release, and piezo coefficients (d_{33}) were, in general, found to decrease with increasing pore former concentration. In addition, Lucite shown to be a more effective pore former to bring the sintered density down than Avicel. More importantly, the probability of premature high-voltage breakdown was found to increase as a function of increasing density as accentuated by fully dense mixed oxide PZT 95/5 ceramics, which exhibited 100% failure during functional testing. Recently, Tuttle and coworkers¹³ performed a comprehensive study on the effect of density on the hydrostatically induced phase transformation behavior of chem-prep PZT95/5 ceramics. The density was controlled systematically through Avicel pore former addition. Physical properties, such as elastic moduli and depoling pressure, were discussed in terms of bulk density, which was then correlated to the characteristics of the pressure induced FE-to-AFE phase transformation. Experimental data obtained from a wide density range (7.11 – 7.78 g/cm³) showed that when a critical volumetric macrostrain (~ -0.40%) was reached, the ferroelectric PZT 95/5 ceramics would transform into the antiferroelectric phase.

2. EXPERIMENTAL PROCEDURE

Niobium modified PZT95/5 powders were prepared by a co-precipitation method.¹⁰ Solutions of lead acetate and Zr, Ti, and Nb alkoxides in glacial acetic acid were mixed to form a clear cation solution. This solution was added to an oxalic acid/n-

propanol precipitant solution to generate the metal oxalate co-precipitate. The resulting precipitate was then filtered, dried, and pyrolyzed at 400°C for 16 hours. The pyrolyzed powder was then ball milled and calcined at 900°C for 16 hours producing a uniform single-phase perovskite material. The composition used for this study was $\text{Pb}_{0.996}(\text{Zr}_{0.953}\text{Ti}_{0.047})_{0.982}\text{Nb}_{0.018}\text{O}_3$ which corresponded to 0.5 mol% of PbO excess of stoichiometry (to compensate for lead loss during processing). Less than 2.5 wt % of pore former was added (data reported in Table 1) to the calcined PZT powder in a 2 quart V-blender (Patternson-Kelly) by tumbling with high speed intensifier bars for 5 minutes. Then the appropriate amount of binder solution (3 wt% acrylic binder) was sprayed into the tumbling powder to granulate the powder. Powder compacts were formed by pressing approximately 70 grams of powder at 14 MPa in a double-acting die and then isostatically pressing the compact at 200 MPa. These compacts were then fired at 750°C for 4 hours with a heating rate of 50°C/hour. This thermal treatment gently pyrolyzed the pore former, creating pores greater than 5 μm in the ceramic body. Detailed processes involved with the large-scale powder synthesis¹⁴ and processing¹⁵ were reported elsewhere.

A triple-inverted crucible technique using chemically prepared PZT 95/5 powders for atmospheric control was used to minimize the lead loss during sintering. All compacts were sintered at a temperature of 1350°C with a 6 hour hold at the soak temperature. The heating and the cooling rates were controlled at 50°C/hour. Typical sintered compact weight losses were less than 0.2%. An Archimedes technique with de-ionized water as the suspension fluid was used to measure densities and the amount of open porosity of the sintered compacts. Details on the ceramic granulation, forming and sintering are reported elsewhere.¹⁵

The sintered compacts were ground and sliced to appropriate size, and silver electrodes were fired onto the ceramics at 600°C for 18 minutes. Samples were hot poled to 30 kV/cm at temperature of 105°C. Acoustic longitudinal and shear velocity measurements were performed using digitized pulse-echo waveforms from which time-of-flight measurements were made through parallel faces of the samples. The elastic moduli were determined from elastic constants calculated from acoustic velocities assuming a transverse isotropic material (calculations were based on the rhombohedral symmetry).

The hydrostatic depoling behavior of the FE-to-AFE phase transformation was investigated at room temperature. Isopar H was used as a pressure transmission fluid. Hydrostatic pressure was increased at a rate of 10.3 MPa per second and an 8 μF capacitor was used to collect the charge released from the depoled ceramic. For a consistent engineering evaluation, the transformation pressure (or depoling pressure) is defined as the pressure where 15 $\mu\text{C}/\text{cm}^2$ of charge has been released from the specimen.

3. RESULTS AND DISCUSSION

3.1 Density, Pore Former, and Bulk Modulus

The average percent theoretical densities (TD: 8.01 g/cm³) of sintered PZT 95/5 ceramics in this study ranged from 86.64% to 93.27% (or 6.914 g/cm³ to 7.471 g/cm³). Density measurements were made on the 70 gram sintered slugs where large samples helped to enhance the measurement accuracy of both the geometric and Archimedes techniques. Table I lists all the sample identities, type of pore former, and bulk densities measured in this investigation.

Young's and bulk moduli of poled and unpoled specimens were calculated based on elastic constants (Table II) determined by the acoustic velocity measurements. Experimental results indicates that both longitudinal and shear velocities decreased as density decreased. Bulk modulus values were calculated from elastic moduli using both Reuss and Voigt averages,¹⁶ for which the differences were less than 1%. The Reuss average bulk moduli will be used to discuss property changes in this reported. The calculated values of Young's and bulk moduli, with sintered densities (% theoretical density or TD) are listed in Table III and Table IV, respectively.

Comparing the unpoled samples, electrical poling has a smaller but still significant effect on mechanical stiffness of the ceramics. For example, the transverse Young's modulus, E_{11} , of 91.96% dense PZT samples (made with Lucite pore former) is 116.0 GPa for unpoled and 113.4 GPa for poled specimens, while E_{33} increased from 116.0 to 117.5 GPa after poling. Thus, poled PZT95/5 ceramics are stiffer in the poling direction and more compliant in the direction transverse to poling. These results are similar to those observed for ceramics near the PZT morphotropic phase boundary, although the difference is not as pronounced. Furthermore, the calculated bulk moduli of poled PZT are, in general, slightly greater than the calculated values for unpoled specimens (Table IV). In addition, the increase in E_{33} and bulk modulus from unpoled to poled ceramics is greater for samples containing Lucite pore former than samples with Avicel. Detailed measurements and a comparison of elastic properties of the same material sintered at different temperatures were reported elsewhere.¹³ Combining the experimental data obtained from previous measurements¹³, the effect of density on the bulk modulus of poled PZT ceramics with Lucite and Avicel pore former is shown in Figure 5. The closed circles and the squares represent the density dependence of bulk modulus for ceramics with Lucite and Avicel pore formers, respectively. To the first order, the bulk modulus monotonically increases with sintered density. In addition, previous bulk modulus measurements as a function of density for PZT 95/5 sintered at different temperature(ref. 13, as shown by the open triangles) are quite consistent our results. Bulk modulus (β) can be described as

$$\beta = -V_o / (\partial V / \partial P)_{v=v_o} \quad (1)$$

where P is the applied pressure, V_o is the pressure-free volume, and $(\partial V / \partial P)_{v=v_o}$ is the compressibility of the material; thus ceramics with lower density are more compressible (or compliant) than higher density ceramics. Within the same density range, the bulk modulus of PZT ceramics with Lucite pore former is always greater than those with

Avicel. Although the fundamental reason underlying this phenomenon is not clear, experimental evidence has shown that there is a pronounced effect of pore former on the depoling characteristics of niobium modified PZT 95/5 ceramics.

3.2 Density, Pore Former and Depoling Characteristics

Figure 6 illustrates the hydrostatic depoling behavior of two specimens with Avicel pore former. These samples were selected from the same batch, because depoling characteristics of PZT 95/5 within the same batch are similar if not identical. Sample A was depoled by pressurizing to 482.65 MPa (as shown by the solid line (a)). The result indicated that the stored polarization on the electrodes was gradually released as the hydrostatic pressure increased to approximately 275 MPa, then with a slight increase in pressure, the remaining stored polarization was suddenly released. In general, the overall depoling behavior was more diffuse than what was seen in Figure 2. To understand the diffuse transformation behavior, sample B was depoled consecutively to four different pressure levels (137.9 (b), 206.85 (c), 275.80 (d), and 482.65 MPa (e)). The depoling behavior from sample B revealed several phase transformation characteristics.

First, even at a relatively low pressure level of 137.9 MPa, upon unloading, some charge was released from the test sample (Figure 6 (b)), indicating that some of the FE material had transformed. The small portion of charge that recovered (illustrated by the reducing of polarization release) upon unloading can be attributed to the hydrostatic piezoelectric effect from the poled PZT material. This effect was especially pronounced for samples containing a high concentration of closed porosity before the pressure reached the phase transformation threshold (see Figure 7). As it is well known that a small increase of pore content in hydrophone transducer materials proves to be an effective method for enhancing the hydrostatic piezoelectric effect.^{17, 18} Below ~ 200 MPa, the bound charge in poled PZT95/5 was gradually released up to $2.9 \mu\text{C}/\text{cm}^2$ as shown in Figure 7. Beyond ~ 200 MPa, the amount of bound charge released increased rapidly indicating the start of the FE-to-AFE phase transformation; and the amount of charge released associated with this process became unrecoverable. However, upon unloading, about $2.9 \mu\text{C}/\text{cm}^2$ of charge was recovered. These observations suggested that the initial charge released below ~ 200 MPa was due to the hydrostatic piezoelectric effect. Furthermore, when a sample has completely transformed to the AFE phase, the hydrostatic piezoelectric effect should disappear and no charge recovery should be observed. The lack of a hydrostatic piezoelectric effect was confirmed as shown by the depoling behavior in Fig. 6 (a) and Fig. 6 (e).

Second, after the sample was consecutively depoled to different stress levels, the phase transformation behavior from FE-to-AFE became progressively sharper (Figure 6 (b), (c), (d), (e), as the slope of polarization release curve became more vertical). Fig. 6 (e) shows a sharp transformation during the final depoling process where the remaining FE phase was transformed into AFE phase and all the stored polarization in the specimen was released. The threshold transformation pressure for the final depoling process was around 275 MPa. It was found that more than half of the FE material transformed into AFE phase when the depoling pressure reached 275 MPa. Experimental results also

showed that during the consecutive depoling process there was a small portion of FE material transformed into AFE upon each loading cycle. This implies that on the microstructural level the mean values of the individual crystallite stress and strain distribution may be greater than for a given externally applied pressure for ceramics that are not fully densified. This increase in microscopic stress and strain may be attributed to stress enhancements in the vicinity of pores as shown by Carroll and Holt.¹⁹

The general depoling behavior for samples with Avicel and Lucite pore former with different sintered densities is illustrated in Fig. 8 and Fig. 9, respectively. For both types of pore former, as density decreases the depoling curves become more diffuse and the vertical portion of the polarization release curve is shifted to a lower pressure. The density dependence of depoling characteristics is not as pronounced as seen in Tuttle et al's study¹³ for ceramic containing Avicel pore former, presumably due to the smaller density range in this study (91.13 to 93.27%). By comparing Avicel and Lucite curves of similar density (e.g. Avicel 91.31% and Lucite 91.96%), it can be seen that the depoling characteristic is more diffuse for ceramics with Avicel than with Lucite pore former. The general behavior of this diffuse depoling characteristic associated with ceramics containing Avicel pore former (i.e., relatively small vertical portion with respect to the polarization release curve) may be attributed to stress enhancements in the vicinity of pores. This local stress enhancement may be sensitive to the geometries (or shape) of the pore former. In particular, an acicular-shaped pore may experience more local stress enhancement than a spherical pore. To help verify this assumption, a comparison of the depoling behavior of ceramics containing different sizes of sphere Lucite pore former²⁰ is shown in Fig. 10, where each sample has a density greater than 91.06 % TD. The average density, pore former size, general dielectric and depoling properties of these materials are summarized in Table V. The baseline PZT 95/5 typically fabricated for the development chem-*prep* v-bar program contains Lucite pore former in the range of 40 to 120 μm (HF955). Results show that the general depoling behavior is rather insensitive to the different pore former size used in these materials. This observation further confirms the importance of pore former shape and the associated local stress enhancement that affects the diffuse depoling behavior.

In addition, the stored charge released during the depoling process (Fig.6 and Fig. 7) decreases with decreasing density which could be attributed to the introduction of zero polarization of pore volume into the ceramics. This observation is consistent for ceramics with either Avicel or Lucite pore former. The polarization release of ceramics containing Avicel and Lucite pore former is shown in Fig. 11. These results were collected from previous studies^{14, 21} from PZT 95/5 batched with TSP39 to TSP52 powders, where compositions and processing conditions¹⁵ were strictly controlled. Within the density range from 7.32 to 7.38 g/cm^3 , the average charge release for ceramics with Lucite pore former is about 2.1% higher than those containing Avicel.

From Fig. 8 and Fig. 9, results indicate that the depoling pressure for the FE-to-AFE phase transformation increases with density. The reason for this phenomenon can be attributed to the modulus increase associated with density change (details will be discussed in the next section). A general comparison of the depoling pressure for

ceramics containing Avicel or Lucite pore former is illustrated in Fig. 12. Results show that within the same density range there is an average 10.7% increase in depoling pressure for ceramics with Lucite pore former than those with Avicel.

Experimental data from this study indicates that ceramics with Lucite pore former exhibit an additional, yet small enhancement of charge output which may improve the high temperature output during functional testing. However, the increase in depoling pressure associated with the Lucite pore former may have a negative impact on the output performance at the end of the shock wave induced phase transformation. A strategy for lowering the depoling pressure, while maintaining the high output, was accomplished by adjusting the chemical composition (Ti/Zr ratio in the batch formulation). Recent experimental results have demonstrated the effectiveness of this new approach.

3.3 Strain Induced FE-to-AFE Phase Transformation

Previously, we demonstrated that as density decreases the bulk modulus decreases (Figure 5), and macroscopically the ceramics become more compressible (or softer); correspondingly the transformation pressure also decreases (Figure 8 and 9). By re-arranging Eq. (1), the volumetric change with respect to the external pressure can be expressed by

$$\partial P = -\left(\frac{\beta}{V_0}\right)\partial V \quad (2).$$

This linear relationship holds up prior to the structural phase transformation. Therefore, as the hydrostatic pressure increases up to the transformation pressure (P_c) the corresponding volume change (ΔV) should be the volumetric strain that is required for the structure phase transformation. Eq. (2), thereby, can be written as

$$P_c = -\left(\frac{\Delta V}{V_0}\right)\beta \quad (3)$$

, where $(\Delta V/V_0)$ is the volumetric strain associated with the phase transformation. Fig. 12 illustrates the relationship between the bulk modulus and transformation pressure for ceramics with different densities and pore formers. Results show a linear correlation between the transformation pressure and bulk modulus, suggesting a constant volumetric strain is associated with the structural phase transformation according to Eq. (3). The positive slope for both Lucite and Avicel containing PZT 95/5 in Figure 13 is a result of a negative ΔV value, where the volume decreases as pressure increases. Based on linear least square curve fitting parameters, the critical volumetric strain to trigger the FE-to-AFE under hydrostatic pressure is in the range of 0.42% to 0.54% (as determined by the slopes in Fig. 13), which is in good agreement with measurements by Zeuch et al¹¹ (Fig. 3). At the atomic scale, as the hydrostatic pressure increases the interionic distance reduces, which can greatly enhance the short-range interactions in the lattice. Hence, when the dipole-dipole interactions in adjacent cells become strong enough, a long-range

ordered FE phase can cooperatively transform into a short-range ordered AFE phase. The concept is consistent with thermally induced structural phase transformation in ceramics and metals in the absence of an external stress where strain change is the dominant factor that triggers the structural phase transformation. Therefore, it is believed that when a critical volumetric strain is reached the dipoles in adjacent cells couple into the AFE phase configuration and release the stored polarization from the electrodes.

4. SUMMARY

Based on a large amount of experimental data, we have observed that a slight change in sintered density has a significant impact on transformation pressure and the amount of charge released during hydrostatic depoling of polarizable deformable PZT95/5 ceramics. Both transformation pressure and charge release decrease with decreasing bulk density. These changes are attributed to the decrease in bulk modulus associated with the decrease in bulk density. Results also show that the shape of the pore former can significantly change depoling behavior. In particular, within the same density range, ceramics with Lucite pore former have a 10.7% higher depoling pressure and a 2.1% increase in charge release than those ceramics with Avicel. In addition, within the same density range PZT 95/5 with Lucite pore former exhibits a higher depoling pressure than Avicel containing PZT because of its higher modulus. Depoling data show that the shape of the pore former might have a profound effect on the local stress enhancements in sintered ceramics, which contributes to a diffused transformation behavior observed for ceramics containing Avicel pore former. Results suggest that the transformation from FE to AFE under a hydrostatic condition is triggered by a critical volumetric strain where dipoles in adjacent cells couple into the AFE configuration and release the stored polarization from the electrodes.

Table I. Sample Identification and Measured Density.

HiFi No.	Sample ID	Pore Former	Bulk Density (g/cm ³)	% of Theoretical Density
HF759	X008382	1.00 wt%, Lucite	7.366	91.96
HF759	X008387	1.75 wt%, Lucite	7.145	89.20
HF759	X008390	2.50 wt%, Lucite	6.914	86.64
DEV 044	X007895	----, Avicel	7.471	93.27
HF643A	X007702	1.80 wt%, Avicel	7.394	92.31
HF635	X007623	1.80 wt%, Avicel	7.314	91.31

Table II. The Effective Elastic Constants as a Result of the Effects of Piezoelectricity.

% of TD		C11 (GPa)		C33 (GPa)		C44 (GPa)		C12 (GPa)		C13 (GPa)	
		Unpoled	Poled	Unpoled	Poled	Unpoled	Poled	Unpoled	Poled	Unpoled	Poled
Lucite	91.96	132.8	133.4	131.3	140.3	48.0	47.8	36.2	40.5	37.1	44.5
	89.20	123.9	124.8	122.2	130.7	44.8	44.7	34.0	37.8	33.8	41.0
	86.64	116.0	116.3	113.9	123.0	42.0	41.7	31.4	35.2	31.4	38.5
Avicel	93.27	130.6	131.8	126.4	135.6	47.5	46.9	34.2	39.0	33.8	42.7
	92.31	126.8	126.2	121.1	128.2	45.7	45.2	33.4	37.0	32.6	39.9
	91.31	122.0	121.6	118.7	125.4	44.5	43.7	33.0	35.5	31.9	37.2

Table III. Young's Moduli of PZT 95/5 Ceramics with Different Densities and Pore Former.

% of TD		Young's Moduli (GPa)			Shear Moduli (GPa)			Poisson's Ratio			
			E ₁₁	E ₃₃		γ ₁₂	γ ₁₃		ν ₁₂	ν ₁₃	ν ₃₁
		Depoled	Poled	Poled	Depoled	Poled	Poled	Depoled	Poled	Poled	Poled
Lucite	91.96	116.0	113.4	117.5	48.2	46.4	47.8	0.22	0.22	0.25	0.26
	89.20	108.5	106.4	110.0	44.9	43.5	44.7	0.21	0.22	0.24	0.25
	86.64	101.5	99.1	103.7	42.2	40.5	41.7	0.21	0.22	0.24	0.25
Avicel	93.27	114.5	112.8	114.3	47.9	46.4	46.9	0.21	0.22	0.25	0.25
	92.31	110.4	108.5	108.7	46.2	44.6	45.2	0.21	0.22	0.24	0.24
	91.31	106.9	105.1	107.8	44.5	43.0	43.7	0.21	0.22	0.23	0.24

Table IV. The Bulk Moduli of PZT 95/5 Ceramics of Different Density and Pore Former.

Pore Former	TD (%)	Bulk Moduli (GPa)			
		Resuss Average		Voigt Average	
		Depoled	Poled	Depoled	Poled
Lucite	91.96	68.61	73.91	68.62	74.01
	89.20	63.70	68.83	63.70	68.90
	86.64	59.35	64.36	59.35	64.46
Avicel	93.27	65.66	71.93	65.67	71.98
	92.31	63.54	68.24	63.58	68.26
	91.31	61.78	65.36	61.79	65.38

Table V. The Average Density, Dielectric and Depoling Properties of PZT 95/5 Ceramics with Different Size of Lucite Pore Former. (Source: TSP39, TSP40, and TSP46).

HF ID	Pore Size (μm)	Density (g/cm^3)	% TD	Remanent Polarization ($\mu\text{C}/\text{cm}^3$)	Coercive Field (kV/cm)	Depoling Pressure (MPa)	Charge Release ($\mu\text{C}/\text{cm}^3$)
955*	40-120	7.305	91.20	30.06	10.28	43.19	30.55
963	15	7.323	91.42	30.10	10.25	43.02	30.81
969	120-165	7.294	91.06	30.12	10.34	42.98	31.06

* Baseline material.

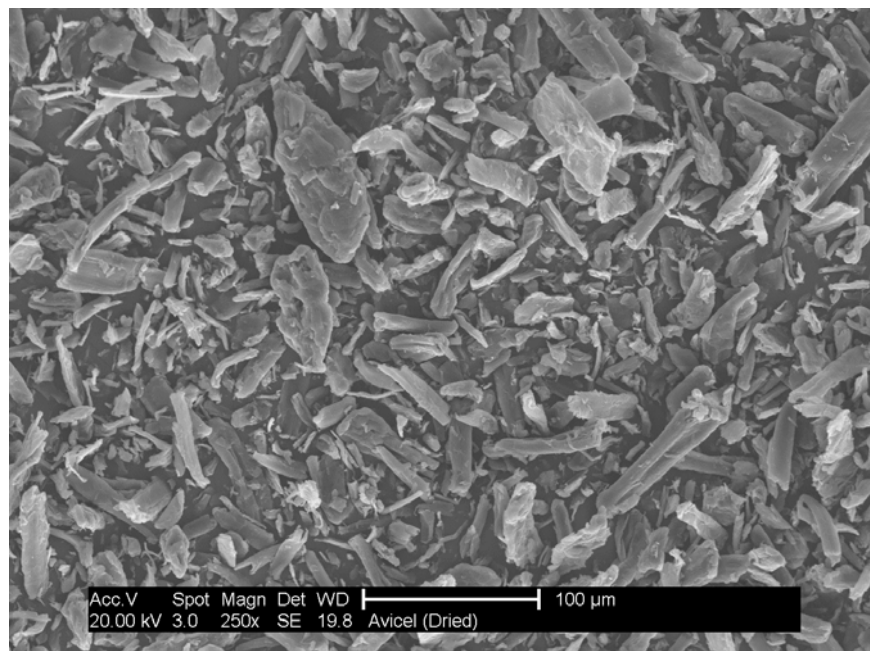


Fig. 1 Microphotography of the Avicel Microcrystalline cellulose.

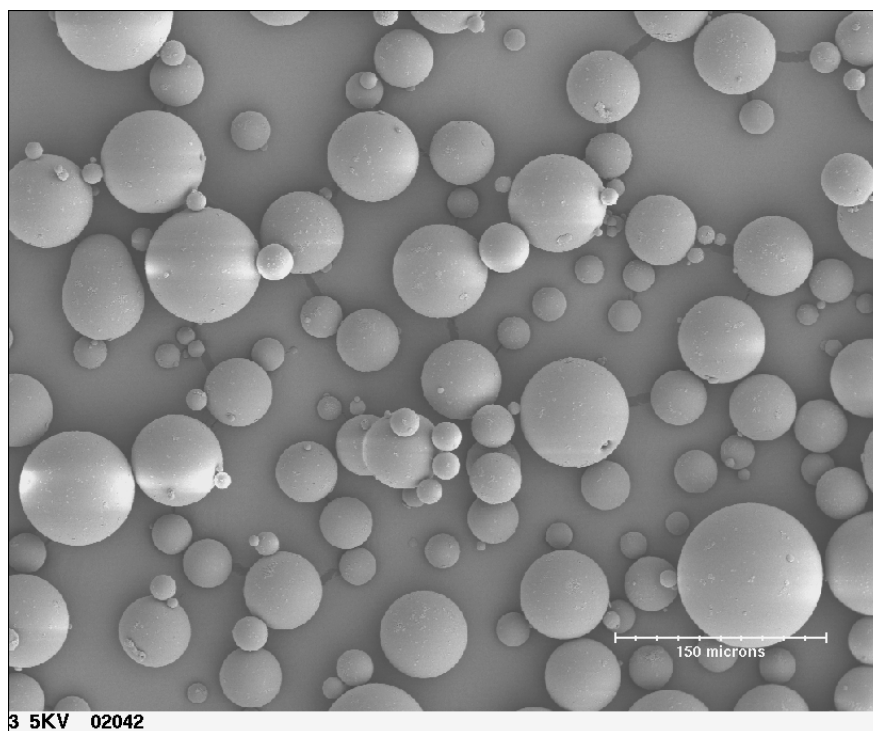


Fig. 2 Microphotograph of Lucite (PMMA), sieved through a 120 mesh screen.

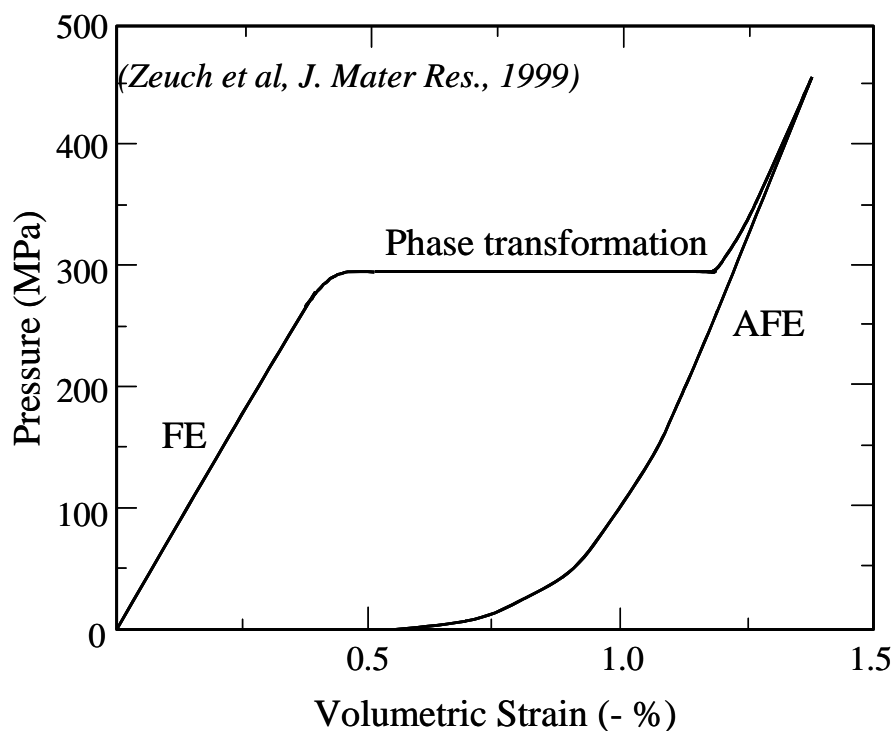


Fig. 3 The pressure-volumetric strain response for the hydrostatically induced FE-to-AFE phase transformation of PZT 95/5 ceramics. (ref. 11)

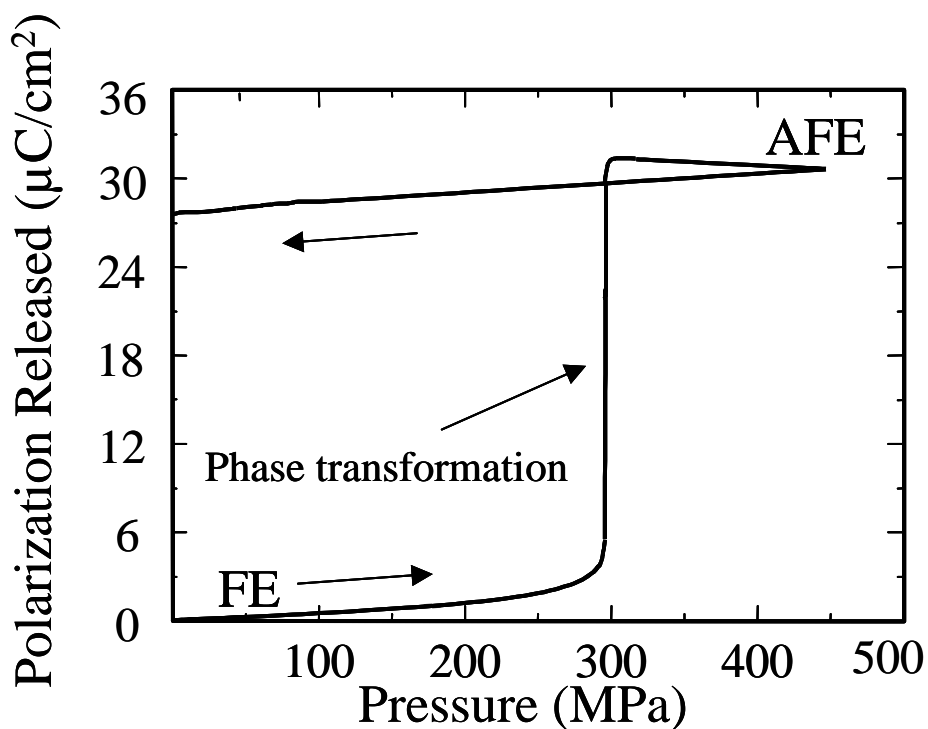


Fig. 4 The polarization release behavior for the hydrostatically induced FE-to-AFE phase transformation of PZT 95/5 ceramics. (ref. 11)

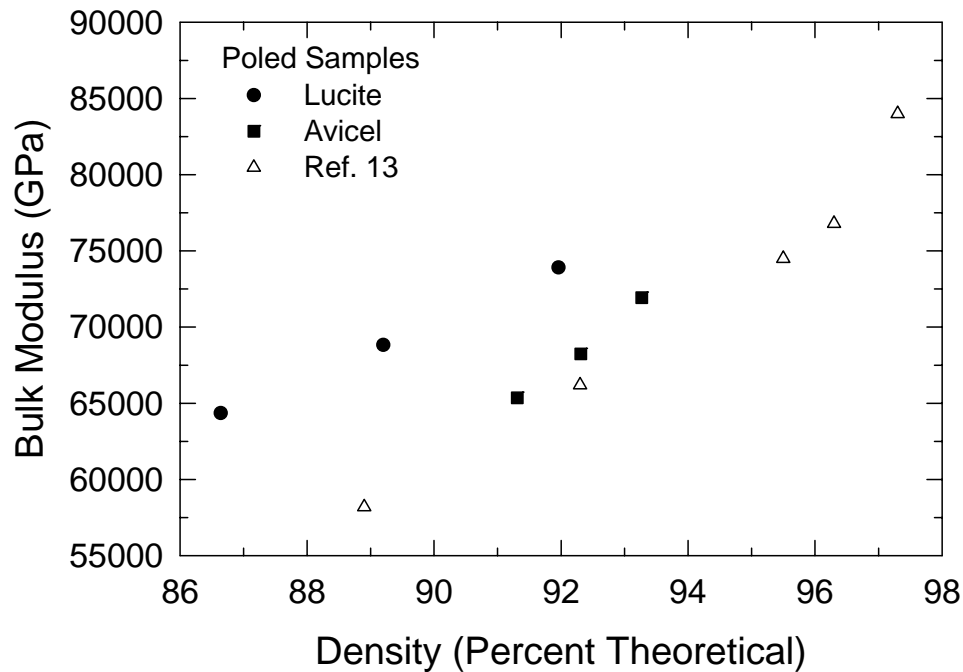


Fig. 5 The effect of density on bulk modulus of poled PZT 95/5 ceramics with different pore formers.

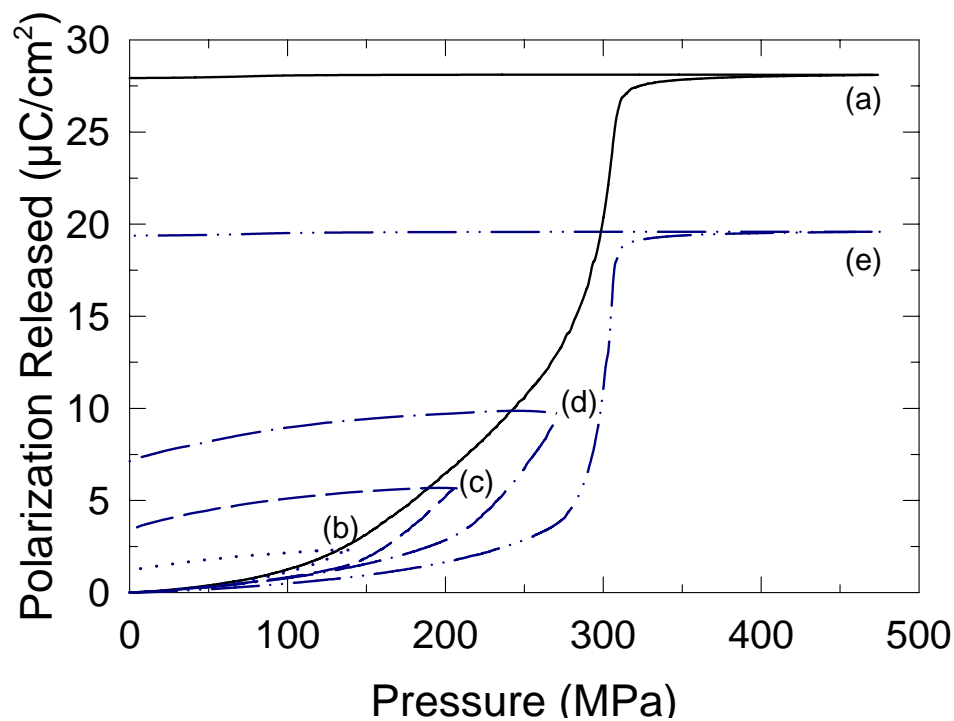


Fig. 6 The depoling behavior of PZT 95/5 with Avicel pore former hydrostatically loaded to (a) 482.65 MPa and unloaded compared with loaded/unloaded sequentially to (b) 137.9, (c) 206.85, (d) 275.80, and 482.65 MPa.

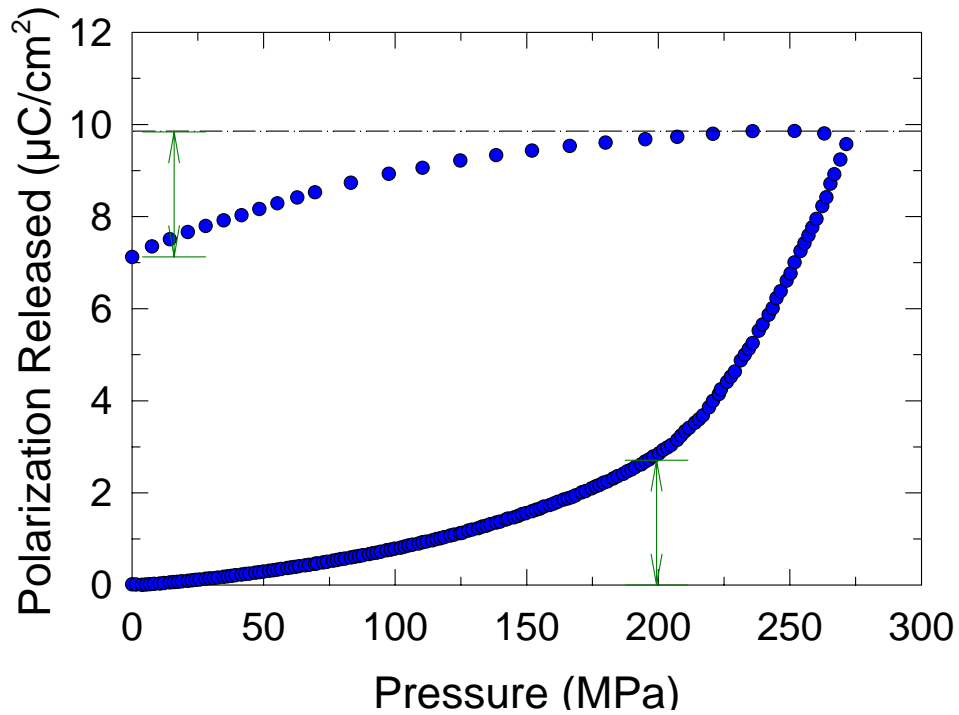


Fig. 7 The amount of polarization released during the loading and unloading cycle below the transformation pressure for Avicel containing PZT 95/5.

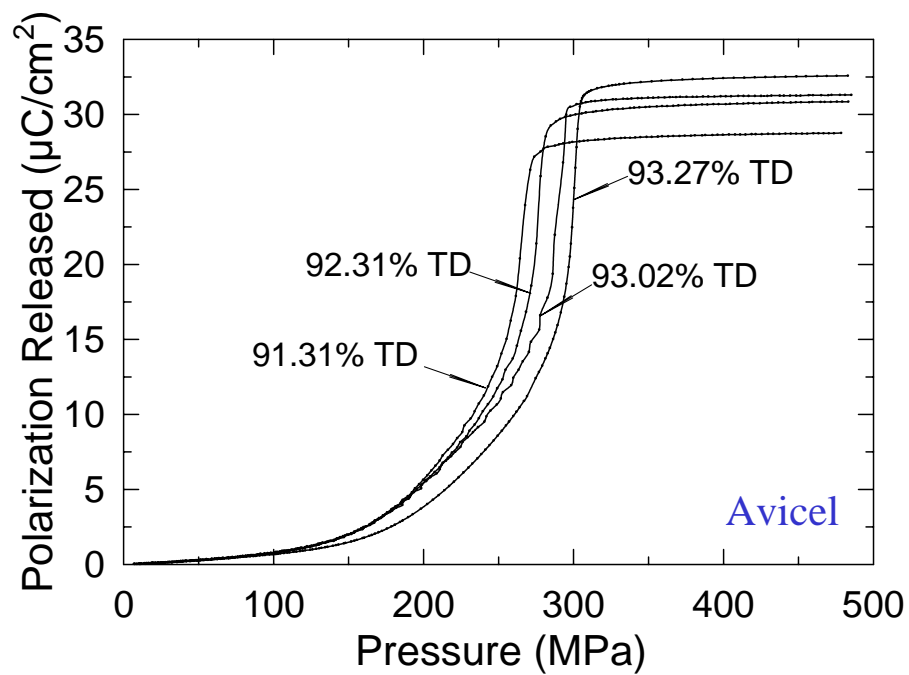


Fig. 8 The general depoling behavior for Nb modified PZT 95/5 ceramics with different densities containing Avicel pore former.

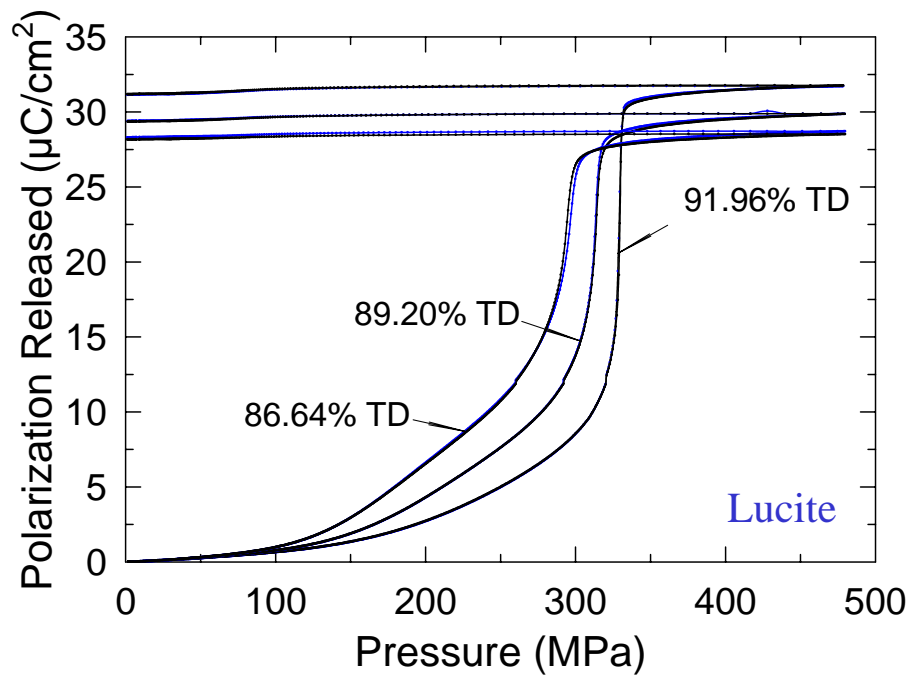


Fig. 9 The general depoling behavior for Nb modified PZT 95/5 ceramics with different densities containing Lucite pore former.

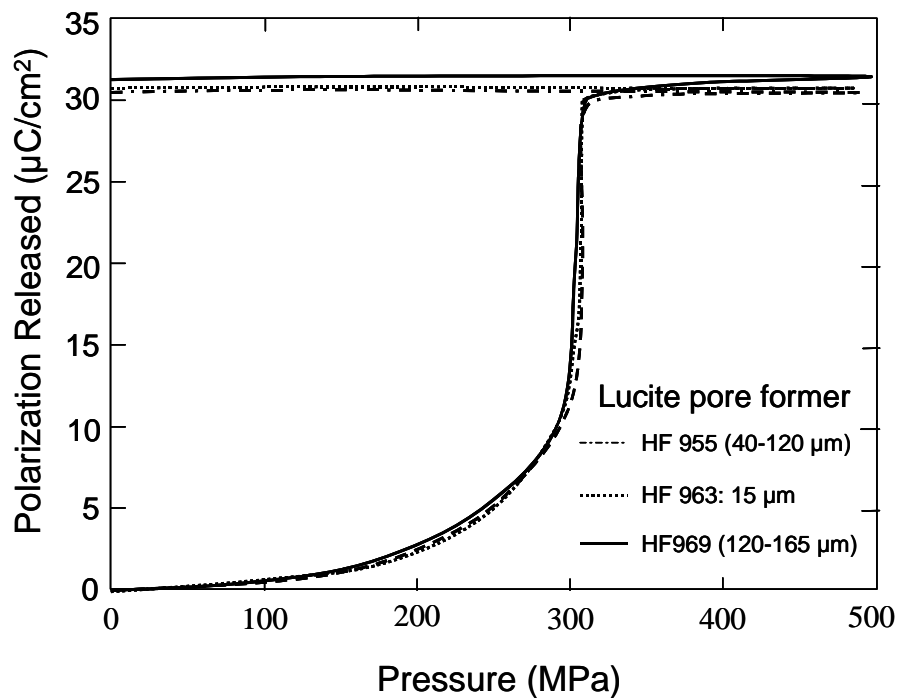


Fig. 10 The depoling behavior for Nb modified PZT 95/5 ceramics with different size of Lucite pore former.

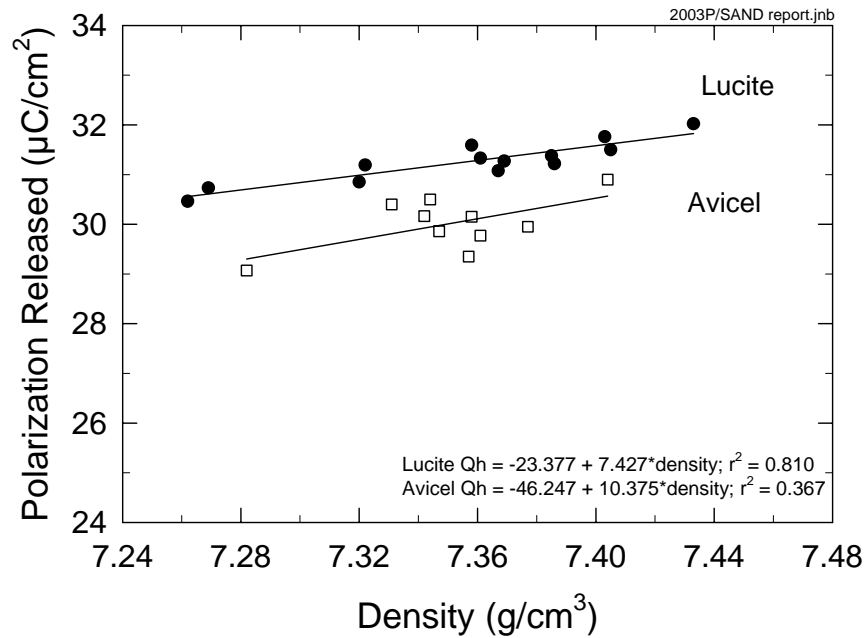


Fig. 11 The amount of polarization release as a function of pore former and bulk density for niobium modified PZT 95/5 ceramics.

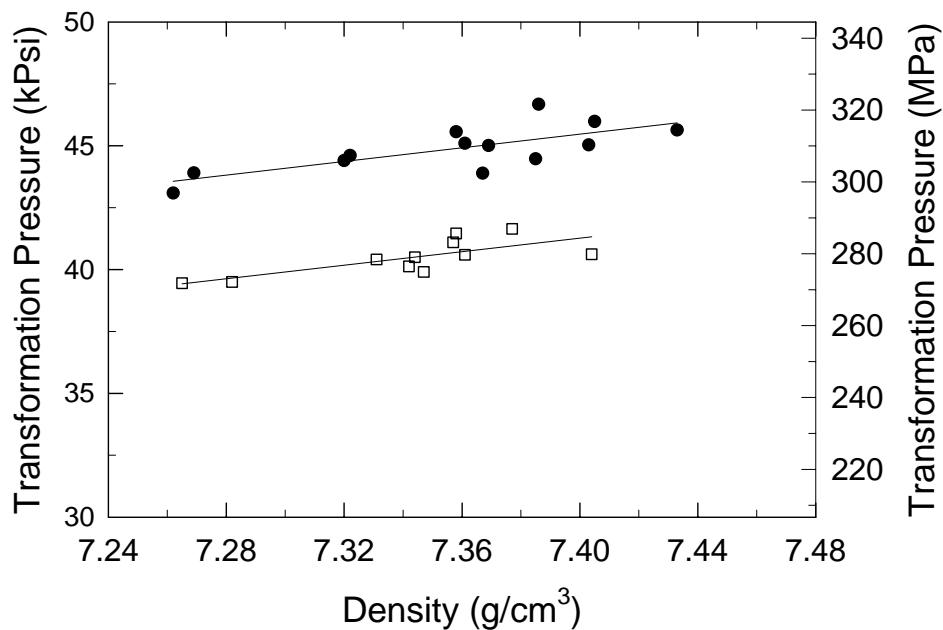


Fig. 12 Depoling pressure as a function of pore former and bulk density for niobium modified PZT 95/5 ceramics.

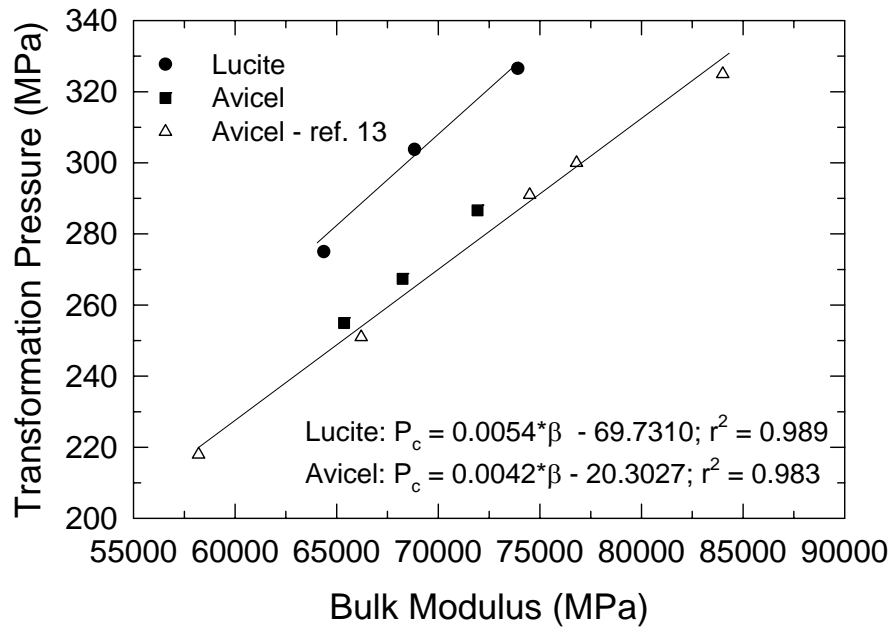


Fig. 13 The correlation between the bulk modulus and transformation pressure for niobium modified PZT 95/5 ceramics with different pore formers.

REFERENCES

- ¹ B. Jaffe, W. R. Cook, and H. Jaffe, in *Piezoelectric Ceramics*, edited by J. P. Roberts and P. Popper (Academic Press, London, 1971).
- ² P. Yang and D. A. Payne, "The Effect of External Field Symmetry on the Antiferroelectric-Ferroelectric Phase Transformation," *J. Appl. Phys.*, **80**, 4001, (1996).
- ³ G. A. Samara and P. S. Peercy, "The Study of Soft-Mode Transitions at High Pressure," in *Solid State Physics: Advances in Research and Applications*, edited by H. Ehrenreich, F. Seitz, and D. Turnbull (Academic, New York, 1981), Vol. 36, p. 1.
- ⁴ P. Yang, J. A. Voigt, S. J. Lockwood, M. A. Rodriguez, G. R. Burns and C. S. Watson, (to be published at Ceramic Transaction Vol. 105, Editor: K. M. Nair; or SAND Report 2003-1511C).
- ⁵ K. Uchino and S. Nomura, "Electrostriction in PZT Family Antiferroelectrics," *Ferroelectrics*, **50**, 191 (1983).
- ⁶ W. Y. Pan, Q. M. Zhang, A. Bhalla, and L. E. Cross, "Field-Forced Antiferroelectric-to-Ferroelectric Switching in Modified Lead Zirconate Titanate Stannate Ceramics," *J. Am. Ceram. Soc.*, **72**, 571 (1989).
- ⁷ P. Yang and D. A. Payne, "Thermal Stability of Field-Forced and Field-Assisted Antiferroelectric-Ferroelectric Phase Transformation in $\text{Pb}(\text{Zr},\text{Sn},\text{Ti})\text{O}_3$," *J. Appl. Phys.*, **71** (3) 1361, (1992).
- ⁸ D. Berlincourt, H. Jaffe, H. H. Krueger and B. Jaffe, "Release of Electric Energy in $\text{PbNb}(\text{Zr},\text{Ti},\text{Sn})\text{O}_3$ by Temperature- and by Pressure-Enforced Phase Transition," *Appl. Phys. Lett.*, **3**, 501, (1971).
- ⁹ F. Bauer, K. Vollrath, Y. Fetiveau, and L. Eyraud, "Ferroelectric Ceramics: Application to Mechanical Electrical Energy Conversion under Shock Compression," *Ferroelectrics*, **10**, 61, (1976).
- ¹⁰ J. A. Voigt, D. L. Sipola, B. A. Tuttle, and M. Anderson, "Nonaqueous Solution Synthesis Process for Preparing Oxide Powders of Lead Zirconate Titanate and Related Materials," U. S. Patent No. 5,908,802, June 1, 1999.
- ¹¹ D. Zeuch, S. T. Montgomery and D. J. Holcomb, "The Effects of Nonhydrostatic Compression and Applied Electric Field on the Electromechanical Behavior of Poled Lead Zirconate Titanate 95/5-2Nb Ceramic During the Ferroelectric to Antiferroelectric Polymorphic Transformation," *J. Mater. Res.*, **14**, 1814, (1999).
- ¹² L. J. Storz and R. H. Dungan, "A Study of the Electrical, Mechanical, and Microstructural Properties of Pb 95/5 PZT as a Function of Pore Former Type and Concentration," SAND Report 85-1312, Sandia National Laboratories, (1986).
- ¹³ B. A. Tuttle, P. Yang, J. H. Gieske, J. A. Voigt, T. W. Scofield, D. H. Zeuch, and W. R. Olson, "Pressure-Induced Phase Transformation of Controlled-Porosity $\text{Pb}(\text{Zr}_{0.95}\text{Ti}_{0.05})\text{O}_3$ Ceramics," *J. Am. Ceram. Soc.*, **84**, 1260, (2001).
- ¹⁴ S. J. Lockwood, E. D. Rodman, S. M. Deninno, J. A. Voigt, and D. L. Moore, "Chem-Prep PZT 95/5 for Neutron Generator Applications: Production Scale-Up Early History," SAND report 2003-0943, Sandia National Laboratories, (2003).
- ¹⁵ R. H. Moore, T. Spindle, and T. V. Montoya, "Chem-Prep PZT 95/5 Neutron Generator Applications: Development of Laboratory-Scale Powder Processing Operations," to be published on SAND Report 2003, Sandia National laboratories, (2003).

-
- ¹⁶ W. D. Kingery, H. K. Bown, and D. R. Uhlmann, *Introduction to Ceramics*, 2nd ed. (John Wiley & Sons, New York, 1976), Chap 15.
- ¹⁷ D.P. Skinner, R. E. Newnham and L. E. Cross, "Flexible Composite Transducers," *Mat. Res. Bull.*, **13**, 599, (1978).
- ¹⁸ W. Wersing, K. Lubitz, and J. Mohaupt, "Dielectric, Elastic and Piezoelectric Properties of Porous PZT Ceramics," *Ferroelectrics*, **68**, 77, (1986).
- ¹⁹ M. M. Carroll and A. C. Holt, "Static and Dynamic Pore-Collapse Relations for Ductile Porous Materials," *J. Appl. Phys.*, **43**, 1626 (1972).
- ²⁰ B. A. Tuttle, D. P. Williams, and W. R. Olson, "Resonance Measurements of Robocast, TSP39,40,46 PZT 95/5 Ceramics with 0.9 Weight Percent Lucite Pore Former Addition of 5 Different Sizes," As a part of pore size study, (Albuquerque, NM: Sandia National Laboratories, August 7, 2002) Memorandum.
- ²¹ S. J. Lockwood, E. D. Rodman, J. A. Voigt and D. L. Moore, "Chem-Prep PZT 95/5 for Neutron Generator Applications: Powder Preparation Characterization Utilizing Design of Experiments," SAND Report 2003-2332, Sandia National Laboratories, (2003).

Distribution

1 MS0886 J.C. Barrera, 01822
1 MS1421 G. A. Samara, 01120
1 MS1421 E. L. Venturini, 01122
1 MS1421 B. E. Setchell, 01122
1 MS0889 S. J. Glass, 01843
1 MS0889 C. S. Watson, 01843
1 MS1411 B. A. Tuttle, 01843
1 MS1349 K. G. Ewsuk, 01843
1 MS1349 W. F. Hammetter, 01843
1 MS1411 J. Liu, 01846
1 MS1411 D. L. Moore, 01846
1 MS1411 J. A. Voigt, 01846
1 MS0515 J. D. Keck, 02561
1 MS0515 P. G. Manley, 02561
1 MS0521 T. W. Scofield, 02561
1 MS0521 S. T. Montgomery, 02561
1 MS1399 M. Lee, 06117
1 MS0819 J. Robbins, 9231
1 MS0959 C. B. DiAntonio, 14192
1 MS0959 T. J. Gardner, 14192
1 MS0959 M. A. Hutchinson, 14192
1 MS0959 S. J. Lockwood, 14192
1 MS0959 T. V. Montoya, 14192
1 MS0959 R. H. Moore, 14192
1 MS0959 E. D. Rodman-Gonzales, 14192
1 MS0959 T. L. Spindle, Jr., 14192
5 MS0959 P. Yang, 14192
1 MS0959 G. R. Burns, 14192
1 MS0867 L. Pope, 14405
1 MS0862 M. E. Gonzales/Allen Parker, 14401
1 MS0871 N. A. Lapetina, 14402
1 MS0869 B. J. Welberry, 14402
1 MS0862 J. A. Wingate, 14401
1 MS0869 M. EL, 14402
1 MS9018 Central Technical Files, 8945-1
2 MS0899 Technical Library, 9616, for DOE/OSTI
1 MS0612 Review & Approval Desk, 9612

2 James Evans,
Room 80, Building D2,
AWE Aldermaston,
Reading, Berkshire RG7 4PR, UK